Journal of Imaging Science and Technology® 50(3): 228–232, 2006.

Color Properties of Specular Reflections

J. S. Arney▲, P. G. Anderson▲, Geoffrey Franz and William Pfeister
Rochester Institute of Technology, Rochester, New York 14623
E-mail: arney@cis.rit.edu

Abstract. *A study has been carried out on the effect of the optical density of inks on the specular reflectance of a printed surface. Samples of cyan, magenta, and yellow ink were printed with a liquid electrophotographic, an offset lithographic, and a thermal transfer printer. Specular reflectance was measured using a goniophotometric instrument to produce the bidirectional reflectance distribution function. The results clearly demonstrated that the amount of specular light reflected from a printed surface depends strongly on the optical density of the ink. A linear correlation was observed between the total amount of specular light reflected from the surface and the square of the transmittance of the ink layer. A highly transparent ink (e.g., yellow ink measured with red light) reflected approximately twice as much specular light than a highly absorbing ink (e.g., yellow with blue or cyan with red). It is suggested that specular reflections from surfaces below the ink layer can contribute significantly to overall specular reflectance of a printed image. © 2006 Society for Imaging Science and Technology.*
[DOI: 10.2352/J.ImagingSci.Technol.(2006)50:3(228)]

INTRODUCTION

When one considers the light that reflects from a printed surface, it is often convenient to parse the reflection process into two types: bulk reflection and specular reflection. In a bulk reflection, the light penetrates to some depth in the ink and paper, and both scattering and absorption occur. Diffusely reflected light is dispersed both in the angle of reflection and in the microlocation of the reflection. The latter is the phenomenon of optical dot gain, or the Yule-Nielsen effect.[1]

Specular reflection is the process responsible for gloss and is generally thought of as a surface reflection largely governed by Fresnel's laws. The magnitude of a Fresnel reflection is governed by the indices of refraction at an interface, such as an air/ink interface. Light absorption is not part of the Fresnel reflection process. Experimentally, specular light is often measured with a gloss meter designed to illuminate and measure at a selected specular angle (equal/opposite angles, $-\theta/\theta$).[2–4] Some angular dispersion of specular light occurs as a result of surface roughness, and goniophotometers are used to measure this angular dispersion. Gloss is generally thought to be the same as the color of the incident light, so the color of specular light is not generally measured.

A goniophotometric instrument described in previous reports[5,6] has been used in the current work to explore specular reflections from images printed with several different processes. Contrary to initial expectation, chromatic effects were found to play a significant role in specular reflections. Further exploration of these effects, as will be shown, has lead to a model of specular reflection that involves Fresnel reflections from multiple surfaces within the printed image.

THE MEASUREMENT TECHNIQUE

Figure 1 is a schematic illustration of the goniophotometric instrument used in the current work. Details of the instrument are described elsewhere,[5] and only a summary is given here. The printed sample is wrapped around a cylinder and illuminated with a line source that is collinear with the cylinder. An electronic camera captures an image of the sample. The camera uses a lens with a long working distance so that parallax from one side of the sample to the other can be ignored. The line light source is sufficiently long and sufficiently far from the cylinder to approximate an infinitely long source at infinity. The light from the source is linearly polarized in the *s* direction. That is, the electric field of the light oscillates in the plane of incidence/reflection. A second polarizer is used as an analyzer in front of the camera lens. Images are captured with both parallel and crossed polarizers, and a difference image is produced. The difference image contains only that light which maintains *s* polarization when it is reflected. The diffuse, bulk scattered light is thereby eliminated from the measurement.[5,7]

An illustration of an image captured with this goniophotometer is shown in Fig. 2. The specular band is clearly

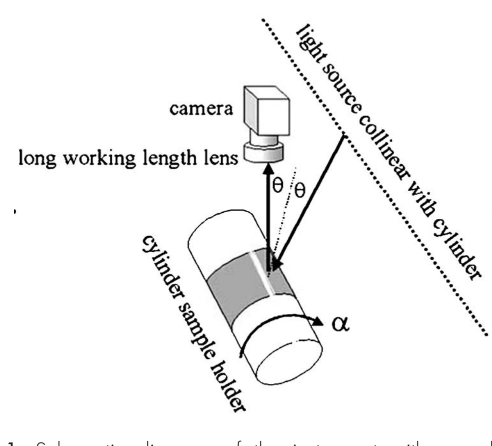

Figure 1. Schematic diagram of the instrument with specular angle =20°. The cylinder is 20 mm, and the camera and illumination distances are sufficiently long to minimize parallax.

▲IS&T Member

Received Sep. 2, 2004; accepted for publication Jul. 5, 2005.
1062-3701/2006/50(3)/228/5/$20.00.

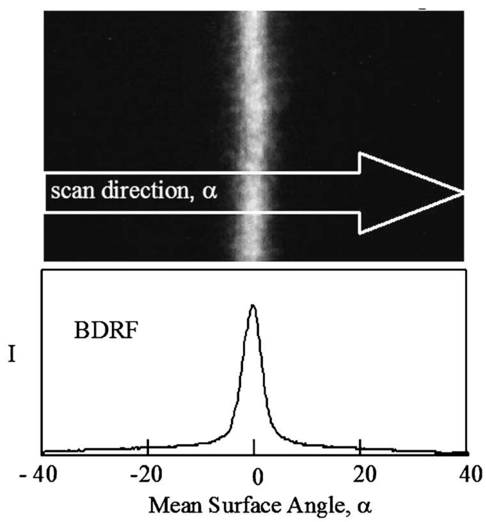

Figure 2. Illustration of an image and a bidirectional reflectance distribution function (BRDF) from the device shown in Fig. 1. The scan direction covers 5 millimeters of the sample.

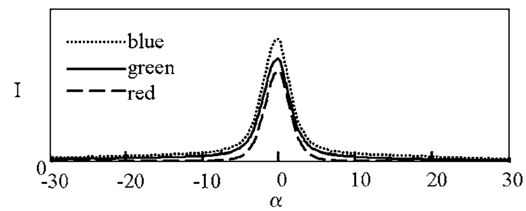

Figure 3. BRDF measured for the cyan ink using blue, green, and red light.

visible, and its angular distribution is calculated from the known geometry of the cylinder. A horizontal scan of this image produces a bidirectional reflectance distribution function, BRDF. The specular lobe is centered at $\alpha=0$, where α is the mean surface angle of the sample.

By measuring light from locations on the sample around the cylinder, the BRDF produced by this device is a measure of reflectance at different sample angles, α, rather than different angles of the source, θ or the detector, $-\theta$, as is more commonly done.[7–10] Surface roughness spreads the specular lobe out over some width in the α direction.[11–13] A complete BRDF analysis would measure the specular lobe in both orthogonal directions, α and β. However, the instrument described in Fig. 1 uses an approximation of an infinitely long light source. As described previously, this averages[5] the specular lobe in the β direction. As a result, the area under the BRDF measured in this way is proportional to the total amount of specular light reflected from the surface.

When a BRDF is measured by scanning the source or detector, each point on the BRDF corresponds to a different Fresnel specular angle, θ. However, by measuring reflectance versus sample angle, α, the resulting BRDF represents the angular distribution of light at a single, fixed specular angle, θ. As a result, the shape of the specular lobe in Fig. 2 is a function only of the topography of the sample, and the area under the lobe is proportional to the total Fresnel reflectance. Experimental verification of this device has been described elsewhere.[5] A specular angle of $\theta=20°$ was used throughout this work.

COLOR IN THE BRDF

A liquid electrophotographic printer (Indigo Ultrastream©) was used to print a solid patch of cyan on a sheet of uncoated, calendered paper of moderately high gloss. The printed sample was mounted on the cylindrical sample holder of the goniophotometer, and measurements were made using light filtered through red, green, and blue filters. The filters chosen for this study were those available in the lab and are approximations of status A filters. As shown in Fig. 3, the BRDF's measured with these different filters show significant differences in curve shape. In addition, the total area under the curve increases in the order red, green, and blue. This suggests that the amount of Fresnel reflected light is greatest for blue light and least for red light for this cyan sample. Samples of solid magenta, solid yellow, and solid CMY black were also printed and measured in this way. Table I shows the integrated areas, r, under the BRDF's expressed relative to the area of the CMY black sample. The areas of the CMY black sample measured with red, green, and blue light were the same within experimental error.

It is evident that the amount of specular light reflected from a printed sample can depend strongly both on the color of the sample and the color of the light. Similar measurements were carried out on samples printed with offset lithography and a thermal transfer printer with similar results, as will be discussed in detail later in this report.

KNOWN WAVELENGTH EFFECTS

In order to rationalize the observations in Table I, two well known wavelength effects were considered. Both effects are based on Fresnel's law of specular reflectance shown in Eqs. (1) and (2).[14] In these equations, ρ_s is the specular reflectance factor for s polarized at $\theta=20°$, the conditions used in the experiments described in this report. The indices n and n' are the indices at the interface where specular reflection occurs

Table I. Relative area, r, under the BRDF for cyan, magenta, yellow, and CMY black inks, printed with an Indigo Ultrastream©, and measured with red, green, and blue light.

	Type of Ink			
	Cyan	Magenta	Yellow	CMY
Color of light	Values of r			
Red	1.2	1.7	1.4	1.0
Green	1.4	1.2	1.3	1.0
Blue	1.5	1.2	1.0	1.0

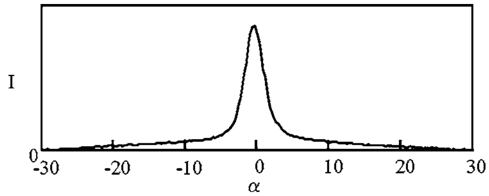

Figure 4. BRDF of the uncoated, calendered paper used as the substrate for the samples printed in this project.

$$\rho_s = \left[\frac{\sin(\theta - \theta')}{\sin(\theta + \theta')} \right]^2, \quad (1)$$

$$\text{where } \theta' = a \sin[n/n' \cdot \sin(\theta)]. \quad (2)$$

It is well known that an increase in the absorption coefficient, ε, of a material results in an increase in the index of refraction, n, of the material, and therefore increase the reflectance factor, ρ_s, at the air/ink boundary. A recent report by Grandberg[15] suggested this effect should increase the specular reflectance of highly absorbing inks. However, the observations summarized in Table I behave in exactly the opposite way. The most highly absorbing combinations (C, M, and Y inks with R, G, and B light, respectively) show the lowest specular reflectance. This suggests that the effect of ε on ρ_s in these systems is overridden by some other effect that acts in the opposite direction.

Another well known effect of wavelength on ρ_s is the ratio between surface roughness and wavelength, σ/λ.[16] This effect reduces ρ_s by a factor of $\exp\{-8[\pi\cos(\theta)\sigma/\lambda]^2\}$ and is a significant factor in the Rayleigh domain ($\sigma \sim \lambda$). However, the effect is monotonic with respect to wavelength, and although it may contribute to ρ_s, it does not rationalize the correlation with absorption maxima observed in Table I.

THE TWO SURFACE MODEL

A possible explanation for the observations shown in Table I is that specular reflections may occur at more than the first surface. Figure 4 shows the BRDF for the unprinted paper substrate used in this work. Comparing the shape of this curve to those in Fig. 3 seems to suggest that the BRDF of the most transparent system (cyan with blue light) might contain a significant contribution from the paper substrate. In other words, it seems reasonable to assume that specular reflections can occur at more than just the first surface, as suggested schematically in Fig. 5.

In Fig. 5, the light must penetrate the ink layer, so the amount of the second surface light, I_2, would depend on the value of the ink transmittance, T. This second surface model predicts that the least amount of specular light would be reflected from the strongest absorbing inks. This is qualitatively in agreement with the data in Table I.

Equations (1) and (2) can be applied to the first surface interface in Fig. 5, with $n = n_1 = 1.00$ (air), and $n' = n_2 =$ the index of the ink. The reflectance factor calculated in this way is ρ_1. These equations can be applied to the second surface

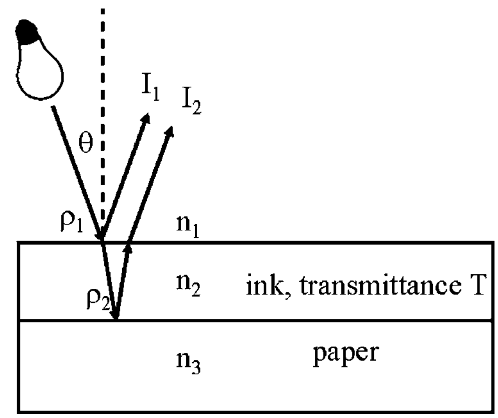

Figure 5. A model of specular reflectance based on reflection from two interfaces.

with $n = n_2$ (ink) and $n' = n_3$ (paper). The reflectance factor calculated in this way is ρ_2, the reflectance at the second surface.

For ordinary organic materials, the $\rho_s \approx 0.04$ at $\theta = 20°$, so fraction $1 - \rho_s \approx 0.96$ passes through the interface into the layer. Similarly, nearly all of the light that returns to the first surface after reflecting from the second surface is transmitted as I_2, and only about 4% reflects back into the ink layer. Therefore, multiple reflections contribute negligibly to the total, and the total reflectance can be estimated by Eq. (3), where T is the transmittance factor of the ink layer and $(1 - \rho_1)$ is the fraction of light that passes through the air/ink interface. Additional internal reflections may occur and would add terms to the right of Eq. (3). However, these terms have been ignored in this model because they contain $\rho_1\rho_2^2$, which is only $\approx 6 \times 10^{-5}$ for $\rho_s \approx 0.04$. In other words, these additional internal reflections are assumed to contribute only a few percent to the total specular reflectance of the system.

$$\rho = \rho_1 + T^2(1 - \rho_1)^2\rho_2. \quad (3)$$

If the CMY black used in the experiments of Table I is strongly absorbing, $T \approx 0$, then the model predicts only a first surface reflectance. Thus, we would expect black to show the minimum specular reflection, $\rho_{\min} = \rho_1$. For a transparent ink, $T = 1$, we would expect the maximum possible specular reflection, $\rho_{\max} = \rho_1 + \rho_2(1 - \rho_1)^2$. Dividing $\rho_{\min}$ by $\rho_{\max}$ gives Eq. (4) for $r_{\max}$, the maximum value of r one would expect to observe in Table I if the model of Fig. 4 applies

$$r_{\max} = 1 + \frac{\rho_2}{\rho_1}(1 - \rho_1)^2. \quad (4)$$

The value of $r_{\max}$ can be calculated by applying Eqs. (1) and (2) to determine ρ_1 and ρ_2 provided that the values of n_1 (ink) and n_2 (paper) are known. If we assume $n_2 = 1.33$ and $n_3 = 4.0$, then we calculate $r_{\max} = 1.7$, which is the largest value observed in Table I. These are clearly unrealistic values for n_2 (ink) and n_3 (paper), but more realistic values signifi-

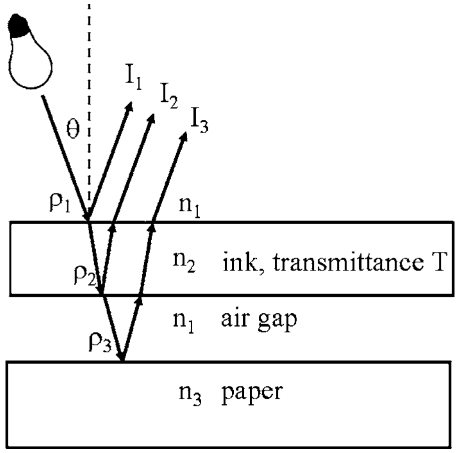

Figure 6. Air gap model of specular reflectance.

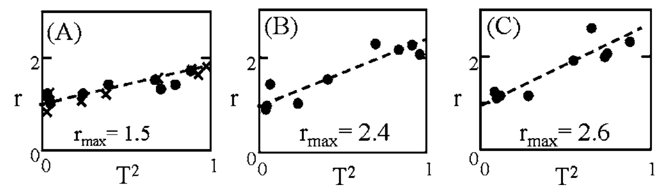

Figure 7. Relative specular reflectance vs T^2 for solid samples of cyan, magenta, and yellow measured in red, green, and blue light, for (a) a liquid EP printer, (b) an offset litho press, and (c) a thermal transfer printer. Data points ● in (a) are from Table I, and × is a duplicate experiment.

cantly underestimate r_{max}. For example, $n_1=1.4$ and $n_2=1.7$ predicts $r_{max}=1.1$. In other words, the two surface model of Fig. 4 does not rationalize the data in Table I.

THE AIR GAP MODEL

In order to rationalize the values of r_{max} in Table I with a two-surface model, the index difference at the second interface must be large. In the air gap model we assume the ink is in optical contact with air, not the paper, as illustrated in Fig. 6.

The air gap model does not assume the ink floats above the paper. Rather, the model assumes the ink is mechanically attached to the paper but does not wet the paper surface and is not in optical contact. An additional consequence of the air gap model is the introduction of a third surface with a significant index difference. This is the interface between the air gap and the paper.

Equations (1) and (2) can be used to show that regardless of the values of n_1 and n_2, the reflectance factors at the first and second interfaces are the same, $\rho_1=\rho_2$. The values of ρ_1 and ρ_3 can be calculated with Eqs. (1) and (2) if the indices n_2, and n_3, are known. Then the total specular reflectance can be modeled by Eq. (5),

$$\rho = \rho_1 + (1-\rho_1)^2 T^2 \rho_1 + (1-\rho_1)^4 T^2 \rho_3. \qquad (5)$$

The reflectance relative to the black sample, $r=\rho/\rho_1$, is Eq. (6),

$$r = 1 + (1-\rho_1)^2 T^2 + (1-\rho_1)^4 T^2 \frac{\rho_3}{\rho_1}. \qquad (6)$$

For $n_1=1$ and reasonable values of n_2 and n_3, Eq. (6) predicts values of $r_{max}>2$. This indicates the air gap model may be reasonable description of specular reflectance of ink on paper.

TEST OF THE AIR GAP MODEL

Equation (6) predicts a linear relationship between r and the square of the ink transmittance, T. The experimental data in Table I can be used to test Eq. (6) if values of T can be estimated. This was done by noting that useful printing inks have negligible scattering coefficients and can be described by the Beer-Lambert law and Eq. (7), where R and R_g are the diffuse reflectance values of the printed sample and the substrate paper, respectively,[1]

$$T = (R/R_g)^{1/2}. \qquad (7)$$

Estimates of T were made by measuring R and R_g using 45°/0° geometry and the same red, green, and blue filters used in the goniophotometer. Figure 7(a) shows the values of r from Table I versus the estimated values of T^2. Figures 7(b) and 7(c) show the results of the same analysis applied to samples printed with an offset lithographic press and a thermal transfer printer. The data in Fig. 7 are consistent with the linear relationship between r and T^2 predicted by the air gap model, and the results are similar for the three different printing technologies used in this work.

The maximum value of specular reflectance, r_{max}, occurs at $T=1$. These values are estimated for the three printing processes in Fig. 6. These values can be compared to the predictions of the model by assuming the values of n_2 and n_3 fall within the range of most ordinary materials, $1.3<n<1.6$. If we assume $n_2=1.3$ and $n_3=1.6$, Eqs. (1), (2), and (6) predict $r_{max}=4.7$. If we assume $n_2=1.6$ and $n_3=1.3$, we calculate $r_{max}=2.1$. The values measured for the offset lithographic and thermal transfer printers might be reasonable for the lower limiting case. However, the observed value of $r_{max}=1.5$ is predicted if we assume $n_2=3.1$ and $n_3=1.3$, which are clearly not reasonable indices for ink and paper. It appears, therefore, that the air gap model significantly overestimates the specular reflectance of printed images.

DISCUSSION

Intuitively, the air gap model seems a reasonable rationale for the chromatic effects seen in the specular reflections of printed materials. In order to fit the model quantitatively to the experimental data, an attenuation factor, F, is added as shown in Eqs. (8) and (9),

$$\rho = \rho_1 + [(1-\rho_1)^2 T^2 \rho_1 + (1-\rho_1)^4 T^2 \rho_3] F, \qquad (8)$$

$$r = 1 + \left[(1-\rho_1)^2 T^2 + (1-\rho_1)^4 T^2 \frac{\rho_3}{\rho_1} \right] F. \qquad (9)$$

With reasonable estimates of $n_2=1.4$ and $n_3=1.5$, and with values of $F=0.5$, 0.8, and 0.8, this model fits the data in Fig.

6 for the three printing processes. We have no direct experimental justification for including the attenuation factor, F, in the model other than the data shown in Fig. 6. Several potential rationales for F might be imagined. For example, the ink might partially wet the substrate and produce a result between complete wetting (two layer model) and no wetting (air gap model). The effect of ε on n and ρ_s may play a role in reducing the value of F. Scattering of light within the ink layer might also decrease the observed value of F. In addition, experimental artifacts such as incomplete separation of the specular and diffuse light through the polarization technique, may play a role. At this point, it is certain only that ink absorbance plays a significant role in gloss.

Experimental values of specular reflectance, r, observed in this work ranged over more than a factor of 2 and correlated significantly with the ink transmittance values, T. Based on these observations, it is somewhat surprising that chromatic effects are not generally noticed when examining the gloss characteristic of printed materials. Perhaps the extreme glint of the gloss coupled with the highly chromatic character of the underlying, diffuse image masks the much lesser chromatic character of the gloss.

ACKNOWLEDGMENTS

This work was sponsored by a grant from Hewlett-Packard Corporation. Special thanks to Norm Burningham for guidance and encouragement.

REFERENCES

[1] Peter G. Engeldrum, "The color between the dots", J. Imaging Sci. Technol. **38**, 545 (1994).
[2] Richard S. Hunter and Richard W. Harold, *The Measurement of Appearance*, 2nd ed. (Wiley, New York, 1987).
[3] Marie-Claude Béland, "Gloss variation of printed paper: Relationship between topography and light scattering", Doctoral thesis, KTH, Royal Institute of Technology, Stockholm, Sweden, 2001.
[4] Per-Åke Johansson, "Optical homogeneity of prints", Doctoral thesis, KTH, Royal Institute of Technology, Stockholm, Sweden, 1999.
[5] J. S. Arney, H. Hoon, and P. G. Anderson, "A micro-goniophotometer and the measurement of print gloss", J. Imaging Sci. Technol. (in press).
[6] J. S. Arney and Hung Tran, "An inexpensive micro-goniophotometry you can build", *Proc. IS&T's PICS* (IS&T, Springfield, VA, 1998) p. 179.
[7] J. C. Stover, *Optical Scattering, Measurement and Analysis* (McGraw Hill, New York, 1990).
[8] I. Nimeroff, "Two-parameter gloss methods", J. Res. Natl. Bur. Stand. **58**(3), 127 (1957).
[9] Standard Practice for Angle Resolved Optical Scatter Measurements on Specular or Diffuse Surfaces, Standard Procedure No. E 1392-96, American Society for Testing and Materials, 1996.
[10] I. Nimeroff, "Analysis of goniophotometric reflection curves", J. Res. Natl. Bur. Stand. **48**(6) (1952).
[11] M.-C. Béland and L. Mattson, "Optical print quality of coated papers", J. Pulp Pap. Sci. **23**, 10 (1997).
[12] H. Rothe and D. Huester, "Application of circular and spherical statistics for the interpretation of BRDF", Proc. SPIE **3141-02**, 13 (1997).
[13] M. A. MacGregor and P. Å. Johansson, "Sub millimeter gloss variations in coated paper, Part 1", TAPPI J. **73**(12), 161 (1990); **74**(1), 187 (1991).
[14] F. A. Jenkins and H. E. White, *Fundamentals of Optics*, 3rd ed. (McGraw-Hill, New York, 1957), p. 509.
[15] Hjalmar Granberg, "Paper optics and perception: Spectral light absorption and gloss of cyan & magenta inks", Acreo Tryckteknisk Forskning, Report No. acr009805, Norrköping, SE (Dec. 2002).
[16] L. Boithias, *Radio Wave Propagation* (McGraw-Hill, New York, 1987).